Supplementary Information (SI) for New Journal of Chemistry.

An Electrochemical Biosensor Based on Glyco-conjugated Cu-BTC MOF for Voltammetric Detection of Bacteria

Deepanshu Bhatt[1,2], Deepak Kumar[1,2], Abhay Sachdev[1,2,*], Akash Deep[3*]

[1] *Materials Science & Sensor Application Division, CSIR-Central Scientific Instruments Organization (CSIR-CSIO), Chandigarh-160030, India.*

[2] *Academy of Scientific and Innovative Research (AcSIR), Ghaziabad-201002, Uttar Pradesh, India.*

[3] *Institute of Nano Science and Technology (INST), Sector-64, Mohali 160062, Punjab, India.*

* Corresponding authors: AS: abhay.sachdev@csio.res.in; AD: akashdeep@inst.ac.in

Buffers used in conjugation

- **Activation Buffer:** 0.1 M MES, 0.5 M NaCl, pH 5.0.
- **Coupling Buffer:** 0.1 M PBS, pH 7.4.

Eq. S1: Randles–Sevcik equation

$$i_{pa} = 0.4961\, nFAC\, ^{2}\sqrt{\left(\frac{n_{\alpha}F\vartheta D}{RT}\right)}$$

$$= 2.99 \times 10^{5}\, n^{2}\sqrt{n_{\alpha}}\, AC^{2}\sqrt{D^{2}}\sqrt{\vartheta}\ (\text{at } 25\ ^{o}\text{C})$$

Where,

$\mathbf{I_{pa}}$ = Anodic peak current,
n = total number of electrons transferred during the redox reaction,
F = Faraday's Constant,
A = Effective surface area,
C = concentration of electroactive species,
D = diffusion coefficient,
ϑ = scan rate

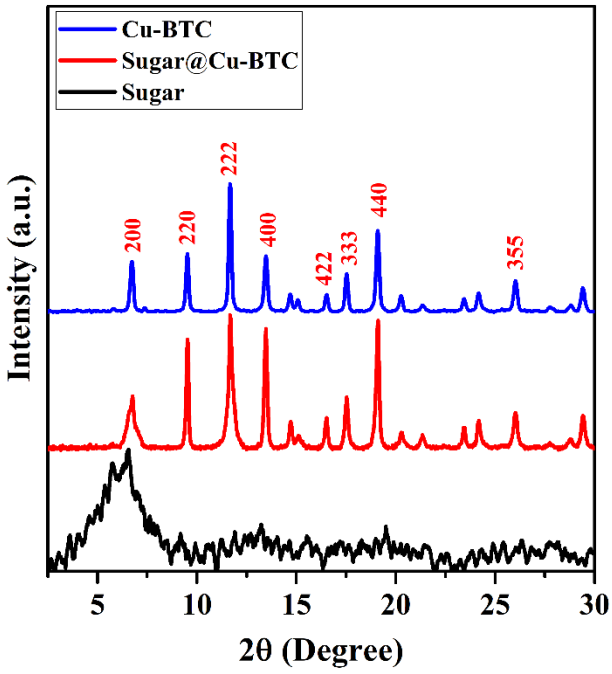

Fig. S1: X-ray diffraction spectra of Cu-BTC, Sugar, and Sugar conjugated Cu-BTC. (**Note:** The sugar used in this study is 4-Aminophenyl-α-D-mannopyranoside (4-APM)).

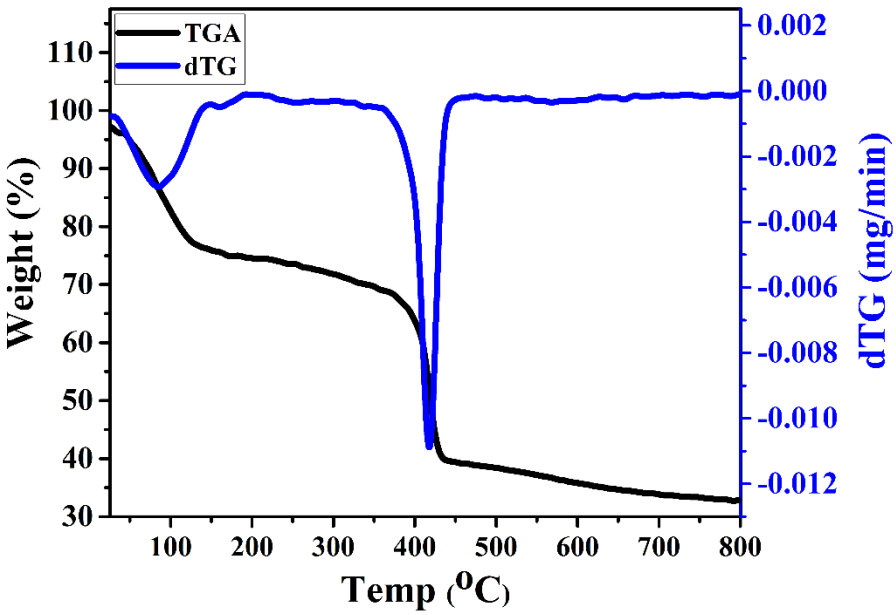

Fig. S2: Thermal Analysis spectra of sugar conjugated Cu-BTC. (**Note:** The sugar used in this study is 4-Aminophenyl-α-D-mannopyranoside (4-APM)).

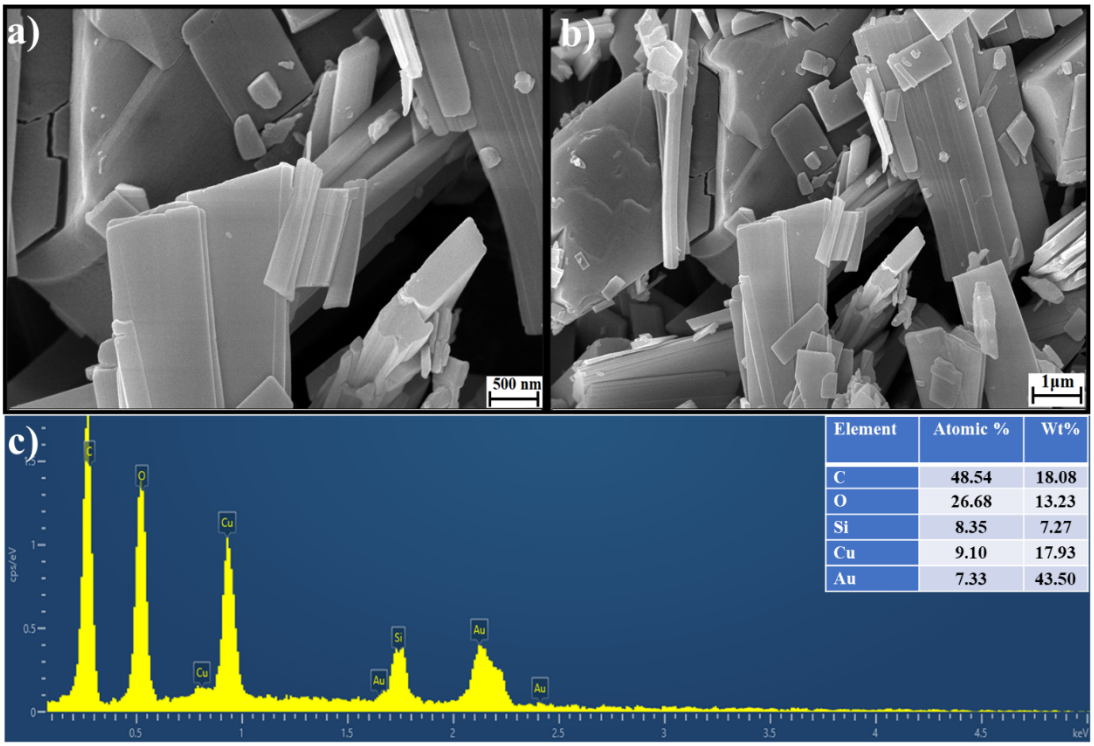

Fig. S3 (a and b): Scanning Electron Microscopy images of sugar conjugated Cu_BTC at different magnifications (500 nm, 1 µm). **(c):** Elemental Analysis Data of sugar conjugated Cu-BTC. (**Note:** The sugar used in this study is 4-Aminophenyl-α-D-mannopyranoside (4-APM)).

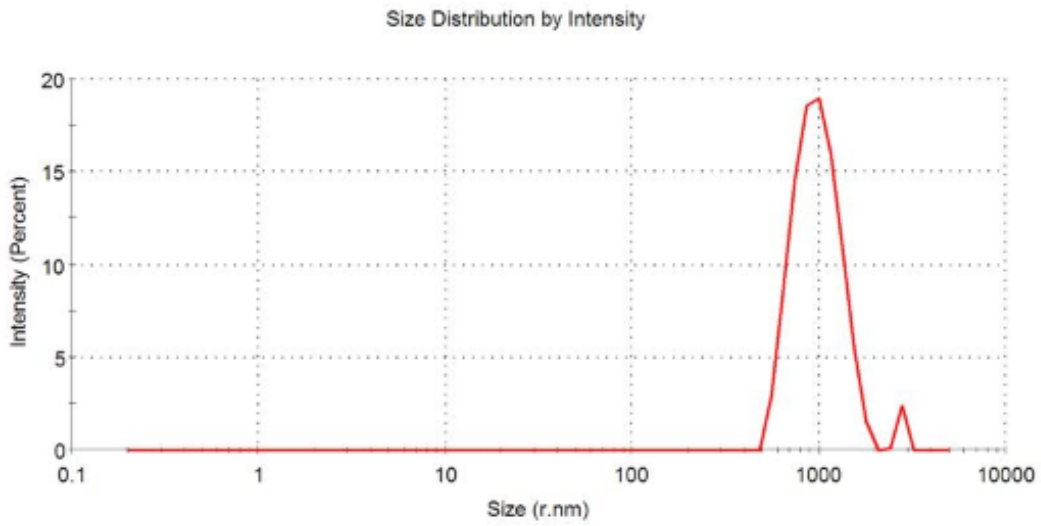

Fig. S4: Size distribution profile for Cu-BTC.

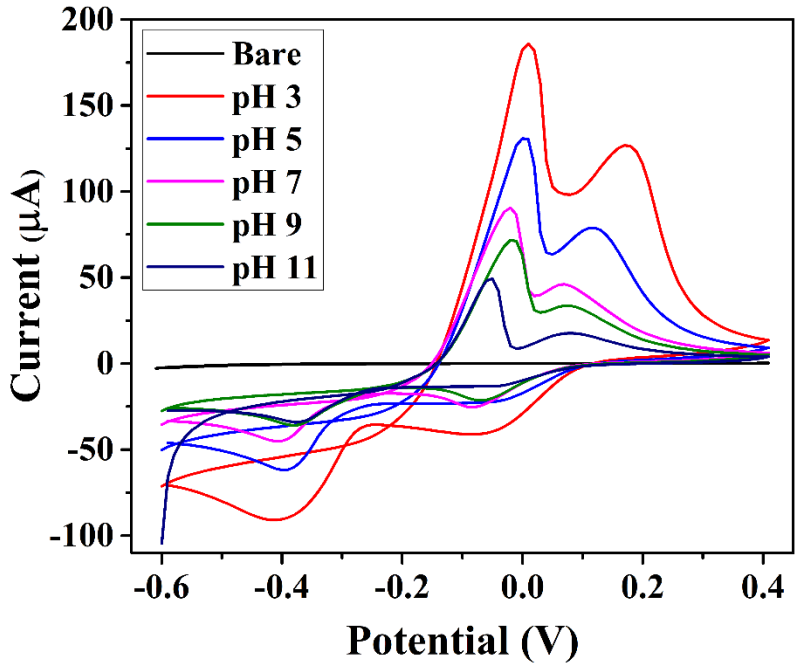

Fig. S5: Cyclic Voltammogram of Cu-BTC/SPCE at various pH solutions of 0.1 M PBS Buffer.

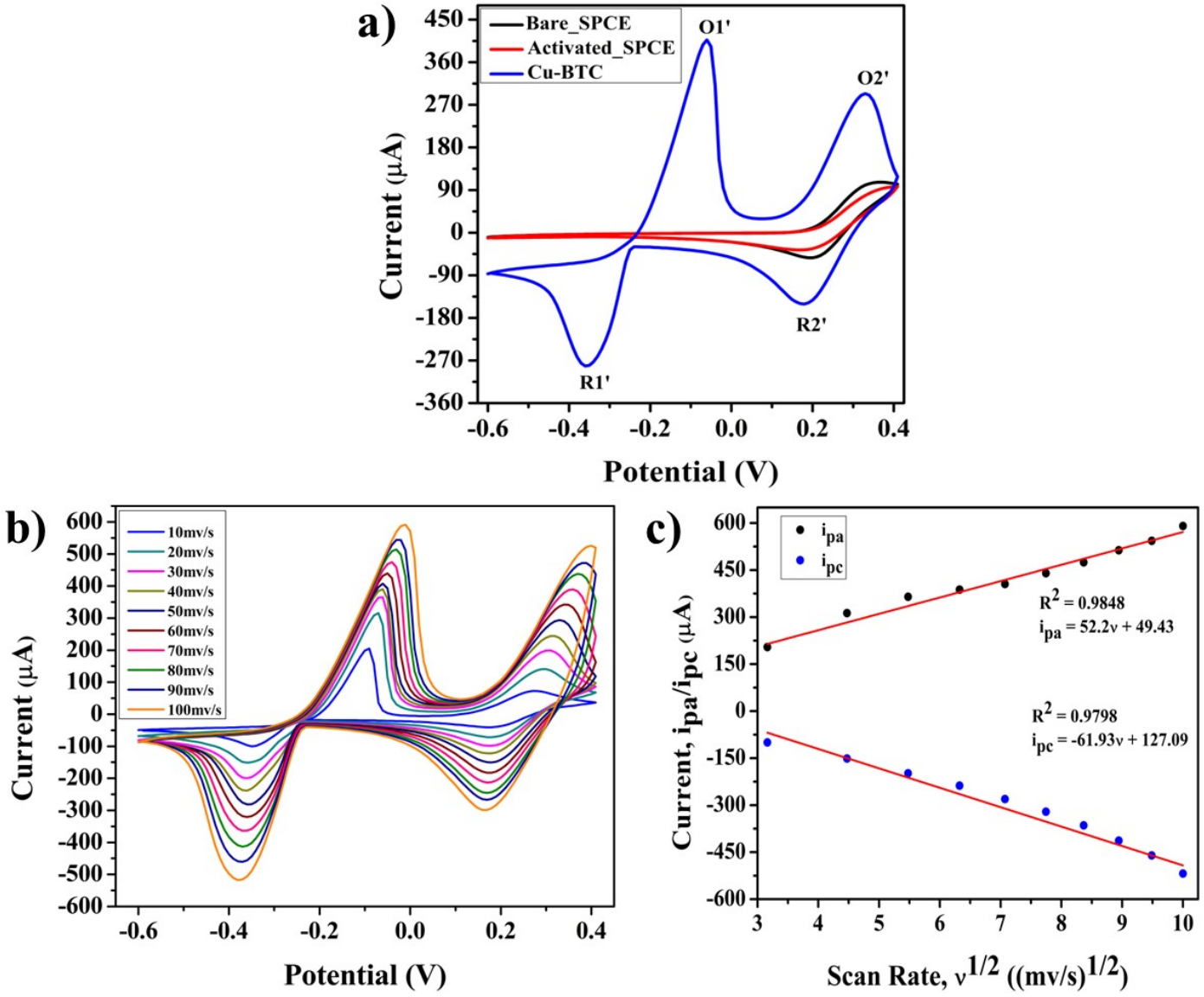

Fig. S6: Cyclic Voltammogram (CV) in $K_4Fe(CN)_6.3H_2O/KNO_3$ in 0.1 M PBS (pH 7.4) electrolyte. **(a):** Graph showing CV of bare SPCE, activated SPCE, and Cu-BTC at 50 mV/s scan rate, **(b):** Graph showing CV of Cu-BTC at different scan rates, **(c):** Graph showing the relationship between the square root of scan rate and oxidation/reduction peak current. **$O_{1'}$, $R_{1'}$:** Oxidation-Reduction pair of Cu(0)–>Cu(I); **$O_{2'}$, $R_{2'}$:** Oxidation-Reduction pair of Cu(I) –>Cu(II).

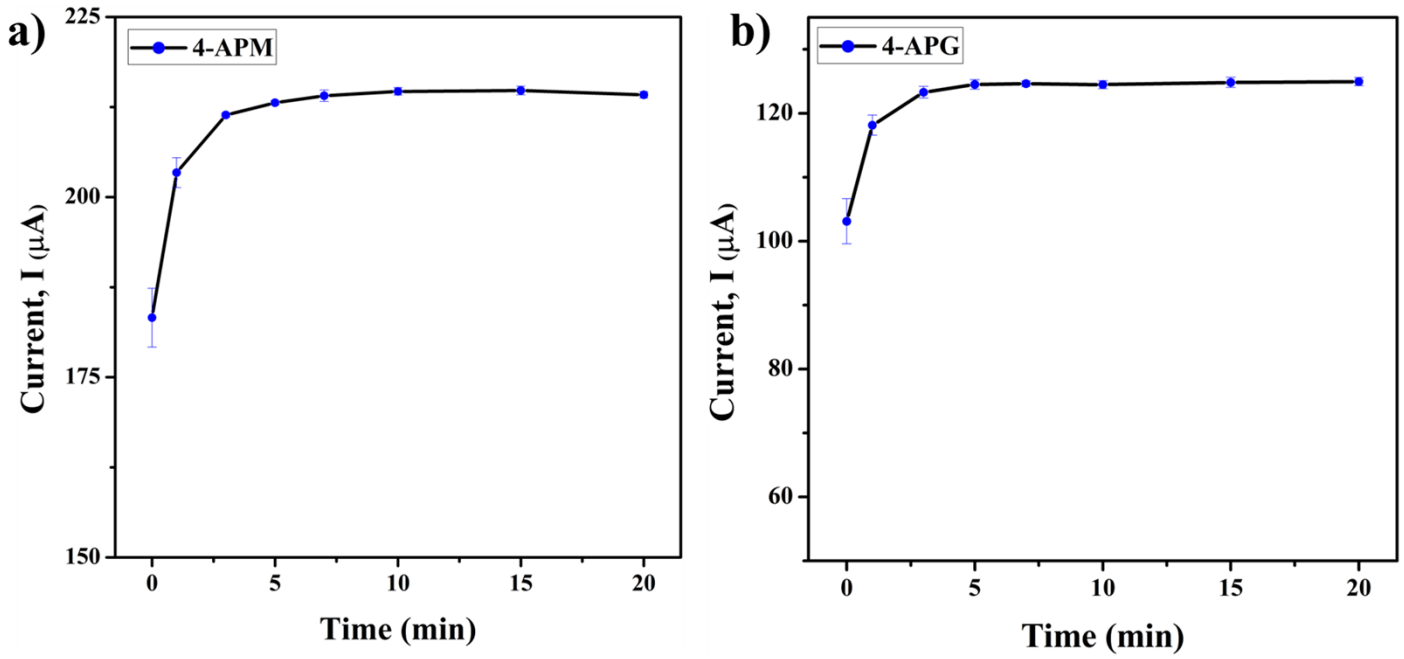

Fig. S7 (a and b): The voltammetric response of the bioprobes measured at various time intervals following the incubation with their respective bacterial analytes.

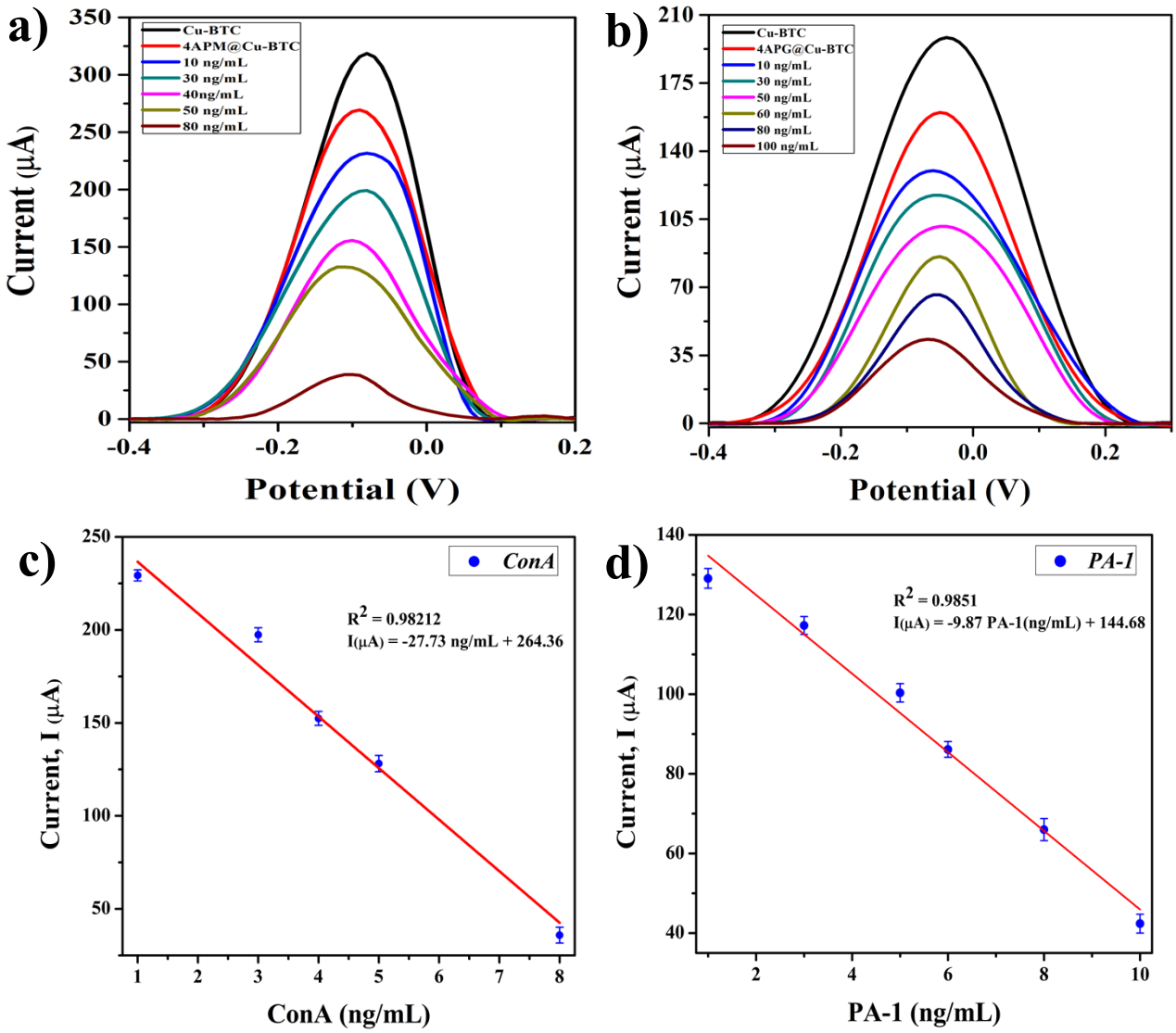

Fig. S8 (a and b): Differential Pulse Voltammetric (DPV) response of 4APM@Cu-BTC and 4APG@Cu-BTC bioprobes as a function of the concentration of ConA and PA-1 lectins, respectively. **(c and d):** Corresponding calibration curves for ConA and PA-1, respectively.

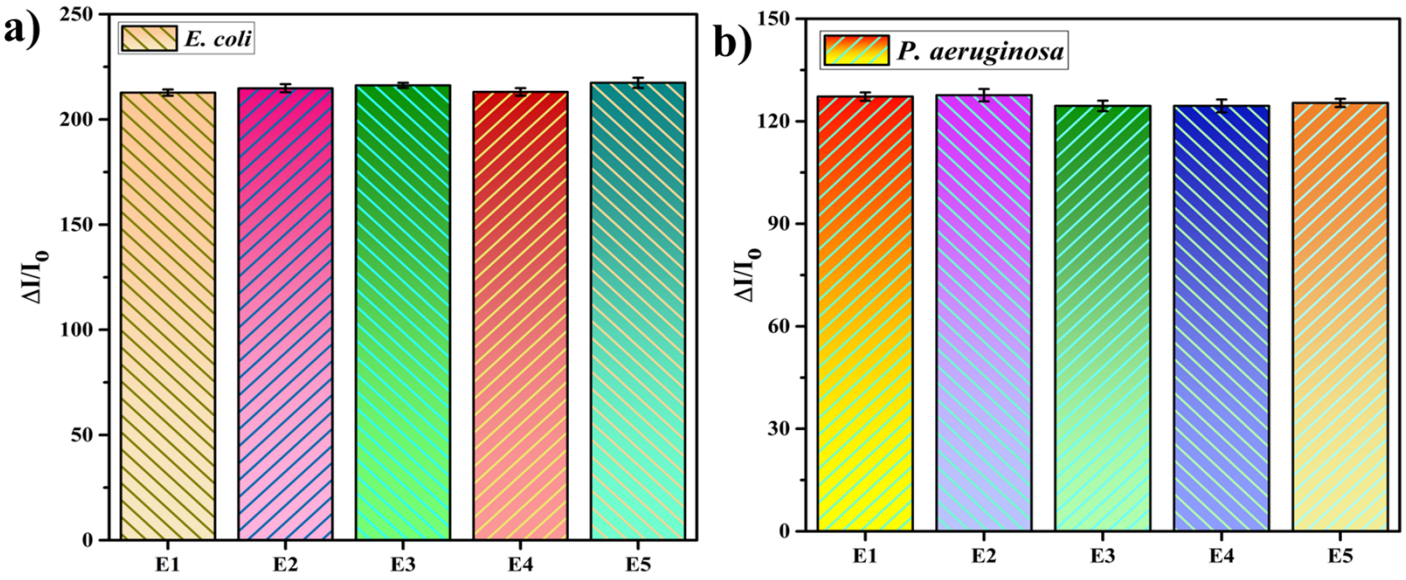

Fig. S9 (a and b): Reproducibility of bioprobes (5 Electrodes, E1-5) under similar conditions.

Table S1: Differential Pulse Voltammetry (DPV) parameters

Potential Window (V)	-0.6 to 0.4
Scan Rate (mV/sec)	50
Amplitude (mV)	100
Pulse (mV)	10
Time of Pulse (msec)	50

Table S2: Analytical performance of as-fabricated bioprobes towards the respective lectins.

Bioprobe	**Sensitivity ($\mu A/ng/mL/mm^2$)**	**Detection Range**	**LOD**	**Analyte**
4-APM@Cu-BTC/SPCE	3.32	10^5 to 10^{10} CFU/mL	2461 CFU/mL	***Escherichia coli***
4-APM@Cu-BTC/SPCE	3.92	10 to 80 ng/mL	27.05 ng/mL	**ConA**
4-APG@Cu-BTC/SPCE	2.70	1 to 10^7 CFU/mL	84.68 CFU/mL	***Pseudomonas aeruginosa***
4-APG@Cu-BTC/SPCE	1.39	10 to 100 ng/mL	30.63 ng/mL	**PA-1**

Limit of Detection **(LOD)** = 3.3(σ/s)
Where σ refers to the standard deviation of intercept, and s refers to the slope of the linear curve

Table S3: Electrochemical biosensing probes utilized for the sensing of *E. coli* and *P. aeruginosa* using monosaccharide sugar as biorecognition element.

Sr. No.	**Bioprobe**	**Sensing principle**	**Limit of detection**	**Linear range**	**Incubation time**	**Ref.**

			E. coli			
1.	Mannose@AuNPs/GCE	Impedance	2 CFU/mL	1.3 x (10^1 – 10^6) CFU/mL	60 mins	1
2.	Mannose@Au-electrode	Impedance	2.5 x 10^3 CFU/mL	1.2 x 10^2 to 2.5 x 10^3 CFU/mL	30 mins	2
3.	Mannose@LPFG	SPR	10^3 CFU/mL	-----	1.5 hrs	3
4.	Derivatized-mannose@Au-electrode	SPR	2.5 CFU/mL	2.5 to 2.5 x 10^5 CFU/mL	10 mins	4
5.	Mannose@FeMOF	Photo-luminescence	8 CFU/mL	19 to 19 x 10^6 CFU/mL	5 mins	5
6.	Derivatized-mannose@Aucoated QCM	Piezoelectric	3.7 and 6.6 CFU/mL	10^3 to 10^6 CFU/mL	-----	6
			P. aeruginosa			
7.	Au@SiO_2-TCPP-GT	Colorimetric	10^4 CFU/mL	-----	15 mins	7
8.	Galactose@FeMOF	Photo-luminescence	8 CFU/mL	170 to 34 x 10^7 CFU/mL	5mins	5

AuNP = Gold Nanoparticle, FeMOF = Iron Metal Organic Framework, QCM = Quartz Crystal Microbalance, SPR = Surface Plasmon Resonance, GCE = Glassy Carbon Electrode, TCPP =Tris (chloroisopropyl) phosphate, GT = Galactose Tripod, LPFG = Long Period Fiber Grating, CFU = Colony Forming Unit

References

1. S. Hargol Zadeh, S. Kashanian and M. Nazari, *Biosensors*, 2023, **13**, 619.
2. X. Guo, A. Kulkarni, A. Doepke, H. B. Halsall, S. Iyer and W. R. Heineman, *Analytical chemistry*, 2012, **84**, 241-246.
3. A. Celebanska, Y. Chiniforooshan, M. Janik, P. Mikulic, B. Sellamuthu, J. Perreault and W. J. Bock, *IEEE Sensors Journal*, 2019, **19**, 11965-11971.
4. I. Yazgan, N. M. Noah, O. Toure, S. Zhang and O. A. Sadik, *Biosensors and Bioelectronics*, 2014, **61**, 266-273.
5. D. Bhatt, S. Singh, N. Singhal, N. Bhardwaj and A. Deep, *Analytical and Bioanalytical Chemistry*, 2023, **415**, 659-667.

6. G. B. Eshun, H. A. Crapo, I. Yazgan, L. Cronmiller and O. A. Sadik, *Biosensors*, 2023, **13**, 337.
7. P. Garg, N. Priyadarshi, M. D. Ambule, G. Kaur, S. Kaul, R. Gupta, P. Sagar, G. Bajaj, B. Yadav and V. Rishi, *Nanoscale*, 2023, **15**, 15179-15195.